STRUCTURAL RELAXATION IN AMORPHOUS SILICON CARBIDE

L. L. Snead and S. J. Zinkle, Metals and Ceramics Division, Oak Ridge National Laboratory, Oak Ridge TN 37830-6138

OBJECTIVE

The objective of this work is to explore the structural relaxation and corresponding physical property changes which occur in amorphous SiC prior to crystallization.

SUMMARY

High purity single crystal and chemically vapor deposited silicon carbide has been amorphized under fast neutron irradiation. The gradual transition in physical properties from the as-amorphized state to a more relaxed amorphous state prior to crystallization is studied. For the three bulk properties studied: density, electrical resistivity, and thermal conductivity, large property changes occur upon annealing between the amorphization temperature and the point of crystallization. These physical property changes occur in the absence of crystallization and are attributed to short, and perhaps medium range ordering during annealing. It is demonstrated that the physical properties of amorphous SiC can vary greatly, and are likely a function of the irradiation state producing the amorphization. The initiation of crystallization as measured using bulk density and in-situ TEM is found to be ~ 875°C, though the kinetics of crystallization above this point are seen to depend on the technique used. It is speculated that in-situ TEM and other thin-film approaches to studying crystallization of amorphous SiC are faulted due to thin-film effects.

PROGRESS AND STATUS

Introduction

Numerous studies [1-10] have shown that SiC becomes amorphous during ion-beam irradiation at 80-350 K for damage levels of approximately 0.1 to 0.5 dpa (displacements per atom.) The majority of studies relating to SiC amorphization have utilized low-energy (<1 MeV) ion-beams [2-7], with a few researchers studying the amorphization threshold using high energy electrons.[11-14] The effect of irradiation temperature on the critical dose required for amorphization has been studied over the temperature range of 77 to 470 K. It has been shown that the critical dose required for amorphization is a function of the irradiation species, irradiation temperature, and irradiation dose rate. Furthermore, the critical dose for amorphization has been shown to consist of at least three sub-stages (dose jumps),[15] attributed to close-pair recombination of three different point defect configurations. Long-range point-defect migration occurs at temperatures above ~350 K in 2 MeV ion irradiated SiC, and amorphization is not possible, even for high dose (>10 dpa) irradiation at temperature above ~ 425 K. [16]

Mechanical properties such as density, elastic modulus and hardness of amorphized single crystal SiC have been previously estimated from measurements of the surface or buried amorphous layers on the ion beam irradiated material. Specifically, the density has been inferred from surface step height measurements [17-19] or by observing the increase in total range with

***Oak Ridge National Laboratory (ORNL) is operated for the U.S. Department of Energy by UT-Battelle, LLC under contract DE-AC-05-00OR22725.**

TEM, [9,10,16,20] or by x-ray techniques [21,22], yielding a density decrease ranging from about -22% to -15%. The residual hardness (H_i/H_u) [10,18,19,23] and residual modulus (E_i/E_u) [10,23] have likewise ranged in the literature from 45%-70% (relative hardness) and 70-76% (relative modulus.)

In previous work by the authors [24], the ability to amorphize silicon carbide using fast neutrons was demonstrated and this material was used for bulk physical property measurements. Physical property measurement using neutron-amorphized SiC offered the advantage of a bulk sample as compared to making measurements on buried or surface amorphous layer inherent in ion-implantation studies. In this way precise crystalline-to-amorphous property change measurements were possible. Specifically, density was seen to decrease by 10.8%, with residual hardness and modulus ratios of 54% and 55%, respectively.

This paper extends this previous work by studying the relaxation of the amorphous SiC (a-SiC) structure occurring prior to the point of crystallization. Such a structural relaxation process has been observed in thin-film amorphous silicon [25] and recently studied in thin film SiC by Wendler [26].

Experimental

Materials for this study were Cree single-crystal 6-H SiC and Rohm Haas chemically vapor deposited (CVD) SiC, which consists of a very high purity, large grain, highly faulted beta (fcc) structure. Major impurity concentrations for the CVD SiC, as supplied by the manufacturer for their standard grade of material in weight parts per billion, are: 70-700 N, 30 Na, <34 Mg, 88 S, <40 Fe, <100 Se, 9 Al, <29 Ga, <22 In, Tl<21, 290 B, 28 P and <27 Sb. The Al, Ga, In, Tl and B act as p-type dopants while the P and Sb act as n-type dopants. These materials were irradiated to fluences of 2.6 and 4.0 x 10^{25}n/m^2 (E>0.1 MeV) in the target region of the High Flux Isotope Reactor at ORNL. These fluence levels are equivalent to 2.6 and 4 dpa, respectively, using a sublattice-average displacement energy of 40 eV. However, it is noted that there will be greater displacements on the carbon sub-lattice as compared to the silicon sub-lattice. The irradiation temperature was ~70°C. A second set of CVD SiC samples, irradiated to the same fluence in the temperature range of 300-400°C, remained crystalline. Amorphization was determination by bright and dark field imaging and the presence of spot-free, diffuse diffraction patterns. Previous work on the 2.6 dpa material using x-ray diffraction and high resolution TEM (HRTEM) was conducted to determine full amorphization. For the case of the HRTEM, there was a complete absence of structure during attempted lattice imaging.

Annealing of each sample was performed in an air furnace for a 30-minute period followed by a 15-minute cleaning in hydrofluoric acid to remove any surface silica formation. Density was measured at room temperature using a density-gradient-column technique [27] using mixtures of tetrabromethane and methylene iodide. The accuracy of the measurement was better than 0.001 g/cc and was found to be reproducible in repeated measurements and consistent for duplicate samples. Microscopy was carried out with a Philips CM-12 microscope and a Gatan *in-situ* annealing stage. TEM samples were prepared by conventional thinning and ion milling at 6 keV, 15°, using a liquid-nitrogen-cooled stage. After foil perforation, the specimens were milled at 3 keV, 9° for 10 m at room temperature to reduce surface amorphization associated with the argon implantation. Thermal conductivity was calculated from a flash thermal diffusivity measurement on 6 mm diameter, 10 mm thick specimens. The specific heat of crystalline SiC was assumed. Electrical resistivity was carried out on 1 x 1 x 25 mm bars of CVD SiC using a four-point probe

technique. [28] A Keithley model 238 source measure unit was used to supply the current and a Keithley model 183 sensitive digital micrometer was used to sense the voltage drop. Due to the large change in resistivity of the sample the applied current was varied to ensure Ohmic heating was not affecting the measurement. The applied current range (and accuracy) was 1 μA (0.05%) and 1 nA (0.3%.) The accuracy for the potential measurement was < 0.1%. Both irradiated and non-irradiated samples behaved in an Ohmic fashion for all applied current levels.

Results and Discussion

As has been pointed in recent reviews on ion-implantation effects in SiC, [17,22,26] the reported temperature for onset of crystallization in amorphous SiC covers a wide range, from 600°C to 1700°C. Various techniques have been employed to study crystallization including Raman spectroscopy, cross-sectional TEM, and RBS. At first glance, there does not appear to be a material, or technique, dependence responsible for this disparity in crystallization temperature. Figure 1 shows previously published work by the authors [24] on the same single crystal material used in the present study. Dark-field images taken during the in-situ TEM foil annealing of the neutron-amorphized single crystal SiC are shown. At an annealing temperature of 700°C contrast points begin to appear (indicated by white arrows in the left image of the figure.) Using through-focus observation and by using comparative analysis these points were associated with surface contamination and grew slowly, and did not appear to expand through the thickness of the TEM foil. Above ~ 800°C crystallite growth occurred at widely spaced intervals between which large, completely amorphous, areas remained. The middle image of Figure 1 shows an example of the growing “stars “ in the bulk SiC. It was observed that the crystallites grew slowly in the ~800-1100°C temperature range, and that the crystallite growth rate was approximately linear with annealing temperature. However, in the annealing step between 1125 and 1150°C, the crystallization kinetics became very rapid, with both faster growth of the existing crystallites and rapid nucleation of new crystallites throughout the amorphous material. The microstructure taken during the rapid crystal growth is indicated in the right-most image of Figure 1. Following a 30 minute annealing at 1150°C, no evidence of amorphous material was found anywhere in the sample. The diffraction rings of this polycrystalline material were indexed to be beta SiC (fcc).

The crystallization of amorphous SiC shown in Figure 1 does not correspond to crystallization inferred from bulk density measurements given in Figure 2. It is seen (figure 2) that the density of a-SiC increased linearly with annealing above the irradiation temperature (~70°C), and at ~ 885°C a dramatic increase in densification occurs restoring the materials to its original crystalline density of ~ 3.2 g/cc. Full density is achieved by ~ 950°C. Furthermore, high resolution TEM for bulk a-SiC annealed below 800°C finds no evidence of crystallite formation. It can be concluded from this result that the temperature of onset of crystallization during bulk-annealing and in-situ TEM are similar (800-875 K,) but due to thin-film or other effects, a higher temperature is required during in-situ TEM examination for complete crystallization to occur.

The density of the 2.6 and 4.0 dpa neutron-amorphized material was 2.857 and 2.845 g/cc, respectively. In relative terms, the higher dose sample underwent a greater density change, –11.2%, compared to the –10.8% change for the lower dose sample. The room temperature density of the amorphous specimens annealed at temperatures just below the onset of crystallization (~885°C) is ~ 3 g/cc (i.e. ~ 6.3% lower than crystalline SiC.)

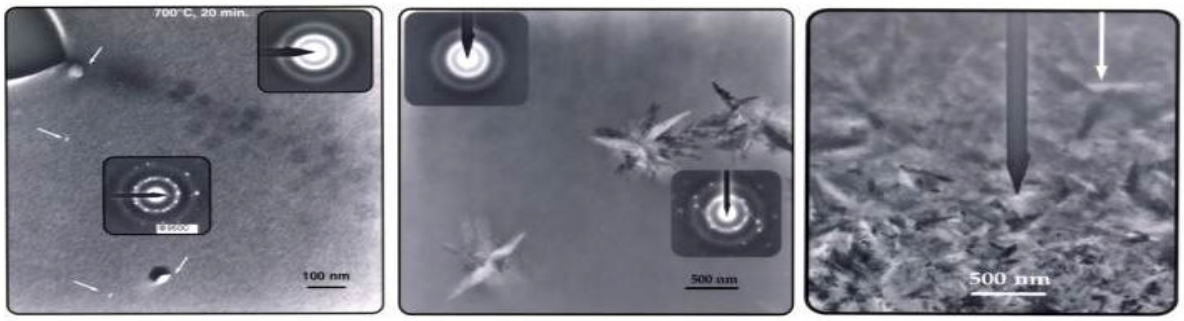

Figure 1. Progression of crystallization in 2.6 dpa neutron amorphized SiC during in-situ TEM annealing.
Left 700°C Middle 950°C. Right, 1150°C.

Changes in the structure of buried (or surface) amorphous layers have been previously observed [17,29] but had been attributed to recrystallization of the discontinuously amorphous, end-of-range region for ion-implanted material. Recently, Wendler [26] measured changes in optical absorption coefficient, refractive index and step-height for a-SiC after annealing at temperatures below the onset of crystallization, and has attributed these changes to a relaxation in the amorphous structure analogous to that occurring in ion-beam amorphized silicon (a-Si.) For the case of a-Si, the presence of vacancy-impurity complexes has been detected by Mossbauer spectroscopy[30]. In addition to this, the effects of annealing on a-Si have been studied using various techniques [25,31-38] proving that the relaxation is intimately related to mutual annihilation of point defects and point-defect complexes in the amorphous material.

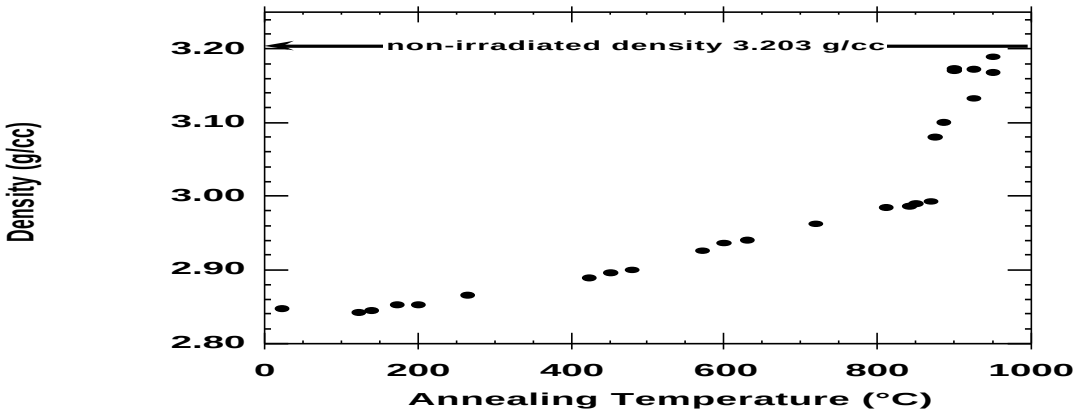

Figure 2. Effect of annealing on the room temperature density of amorphous SiC.

The effect of annealing on the electrical resistivity of crystalline and amorphous SiC are given in Figures 3 and 4. The left plot in figure 3 shows the temperature dependence of electrical resistivity for non-irradiated CVD SiC and the electrical resistivity below the amorphization temperature for the a-SiC. For both the non-irradiated and amorphized conditions, the resistivity is seen to follow $1/T^{1/4}$ dependence, indicative of hopping conduction[39]. Following the analysis performed on a-Si, the defects associated with structural vacancies (dangling bonds) in the random network increases the density of mid-gap states, thus increasing the electrical conductivity, which will be greatly affected by annealing. This is clearly shown in annealing plot of figure 3 which shows the electrical resistivity of a-SiC increasing by ~ 3 orders of magnitude prior to crystallization. It should be noted that upon reaching 885°C, the energy release associated with the crystallization is rapid and sufficient to cause the bulk samples to energetically fracture within the annealing furnace.

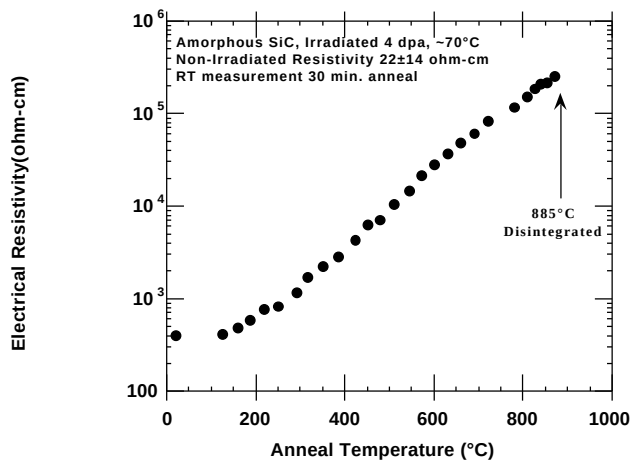

Figure 3. Temperature dependence and the effect of annealing on the electrical resistivity of amorphous SiC.

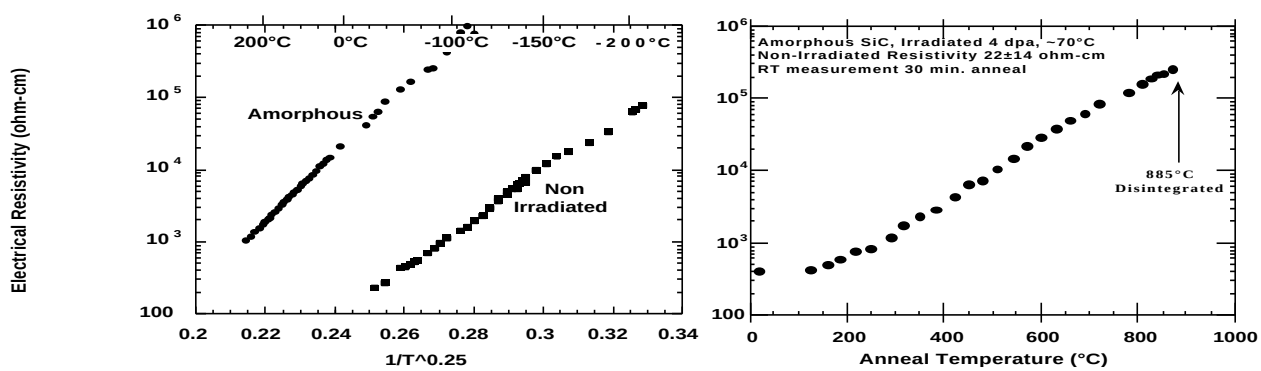

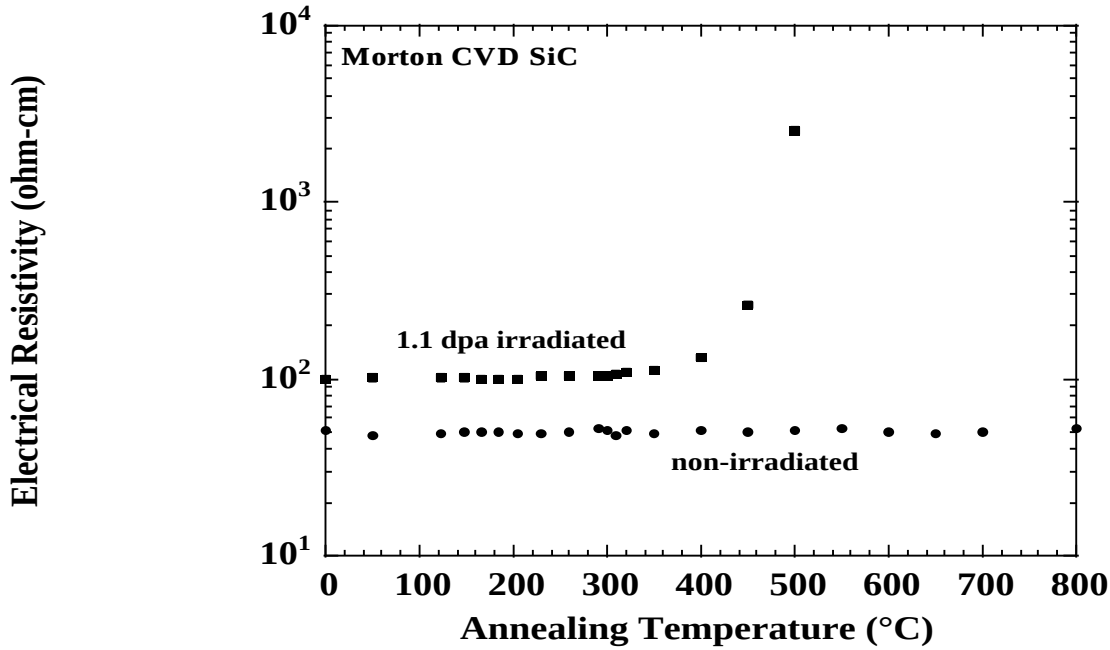

Figure 4. Effect of annealing on the room temperature electrical resistivity of 1.1 dpa damaged crystalline CVD SiC.

The effect of annealing on electrical conductivity of a-SiC can be compared with that of neutron damaged crystalline SiC. Figure 5 shows the electrical resistivity as a function of annealing temperature for CVD SiC, both in the non-irradiated and 1.1 dpa, ~350°C, irradiated condition. The non-irradiated, crystalline material shows constant electrical resistivity of ~50 Ω-cm following annealing up to 800°C. No change was expected as the processing temperature for CVD SiC is in excess of 1000°C. A small resistivity increase is seen for the 1.1 dpa as-irradiated condition. Several competing factors contribute to the change in the as-irradiated resistivity of crystalline SiC. For example, nuclear transmutation doping will occur, increasing the donor concentration through the $^{30}Si(n,\gamma)^{31}Si$, and subsequent beta decay to (n-type donor) ^{31}P. Additionally, 20% of the 290 wppm intrinsic (p-type acceptor) boron would have been removed due to the $^{10}B(n,\alpha)\ ^{7}Li$ reaction. The elastic collisions between high-energy neutrons and the lattice will also produce simple point defects, increasing the dangling bond density, hence decreasing the material resistivity. Upon annealing of the damaged crystalline SiC, simple point defect migration will remove these dangling bonds increasing the resistivity. From figure 4, the resisitivity is seen to asymptotically increase as the annealing temperature exceeds the irradiation temperature, releasing shallowly trapped interstitials or possibly mall point defect clusters.

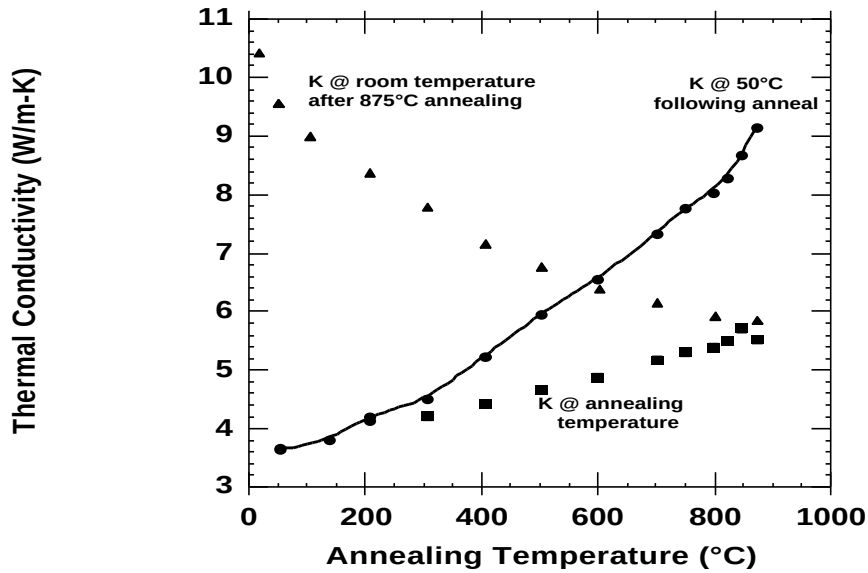

Figure 5. Effect of annealing on the thermal conductivity of amorphous SiC. Solid curve represents thermal conductivity at 50°C. Solid squares are thermal conductivity at measurement temperature. Solid triangles are room temperature thermal conductivity following 875°C anneal.

The thermal conductivity of a-SiC measured at 50°C is also seen to dramatically increase with annealing temperature. Figure 5 shows an increase from an as-amorphized value of 3.6 W/m-K to 9.1 W/m-K following annealing up to 875°C. Following each annealing step, the thermal conductivity was measured during cool down and is plotted at the annealing temperature (solid squares in Figure 5.) The room temperature thermal conductivity at the most relaxed state (following the 875°C anneal) is also shown. At 885°C the sample energetically fractured into small pieces. It is interesting to note that the room temperature thermal conductivity in the most relaxed state for a-SiC (~10 W/m-K following the 875°C anneal) is nearly identical to the saturation value for CVD SiC irradiated above the critical temperature for amorphization (i.e. still crystalline.) The non-irradiated room temperature thermal conductivity for the CVD SiC in this study is 333 W/m-K. Irradiation at 300°C appears to reach saturation thermal conductivity by 0.1 dpa at a value of 11 W/m-K. However, the density of the most relaxed a-SiC (~3.0 g/cc after annealing at ~865°C) is substantially less than the highly damaged crystalline material (3.16 g/cc.) In both materials, the temperature dependence of thermal conductivity indicates that phonons are the primary thermal transport mechanism (also obvious from the electrical resistivity data shown in figure 3.) For crystalline materials, vacancies and their associated strain fields substantially reduce thermal conductivity. Upon annealing of the damaged crystalline material, thermal conductivity is increased substantially. The mechanism behind the recovery process of thermal transport for both the amorphous and damaged-crystalline SiC is similar. For the crystalline material, vacancies and their associated strain fields are reduced as interstitials become mobile. In the case of the amorphous material, the local perturbation in the strain field associated with distorted, or non-existent, bonds act as phonon scattering centers. Clearly, increasing the short-range order in the a-SiC during annealing will reduce phonon-defect interaction and increase thermal conductivity as seen in Figure 5.

CONCLUSIONS

The as-amorphized density of silicon carbide is seen to depend on applied dose and to be function of post-irradiation annealing temperature. This suggests an irradiation-temperature dependence of density (as well as electrical and thermal properties.) Annealing of the amorphous SiC above the amorphization temperature leads to an increase in the bulk amorphous density of ~5%, reaching a value of ~ 3 g/cc at ~ 885 °C, at which point the structure explosively crystallizes. The densification of the amorphous SiC is attributed to annealing out local strain in the amorphous network similar to that seen in amorphous Si. Results on the increase in electrical resistivity and decrease in thermal conductivity of the amorphous SiC during annealing further reinforce this point. Specifically, annealing strained local bonds, or completing the local bonding will reduce the density of mid-gap states increasing electrical resistivity while a reduction in phonon-scattering vacancies (or a reduction in the local strain in the amorphous network) act to enhance thermal conductivity.

REFERENCES

[1] D.P. White, J. Appl. Phys 73 (1993) 2254.
[2] R.R. Hart, H.L. Dunlap, O.J. Marsh, Radiat. Eff. 9 (1971) 261.
[3] J.M. Williams, C.J. McHargue, B.R. Appleton, Nucl. Instrum and Meth. 209/210 (1983) 317.
[4] J.A. Spitznagel, S. Wood, W.J. Choyke, N.J. Doyle, J. Bradshaw, S.G. Fishman, Nucl. Instrum. Meth. in Phys. Res. B16 (1986) 237.
[5] J.A. Edmond, R.F. Davis, S.P. Withrow, K.L. More, J. Mater. Res. 3 (1988) 321.
[6] N.G. Chechenin, K.K. Bourdelle, A.V. Suvorov, A.V. Suvorov, A.X. Kastilio-Vitloch, Nucl. Instrum. and Meth. in Phys. Res. B65 (1992) 341.
[7] L.L. Horton, J. Bentley, L. Romana, A. Perez, C.J. McHargue, J.C. McCallum, Nucl. Instrum. Meth. in Phys. Res. B65 (1992) 345.
[8] W.J. Weber, L.M. Wang, N. Yu, H.J. Hess, Mat. Sci. Eng. A253 (1998) 62.
[9] L.L. Snead, S.J. Zinkle, in: MRS Symposium on Microstructure of Irradiated Materials eds. I.M. Robertson et al., vol. 373 (MRS, Pittsburgh, 1995) p. 377.
[10] W.J. Weber, N. Yu, L.M. Wang, N.J. Hess, J. Nucl. Mat. 244 (1997) 258.
[11] H. Inui, Phil. Mag. B 65 (1992) 1.
[12] H. Inui, H. Mori, T. Sakata, Phil. Mag. B 66 (1992) 737.
[13] H. Inui, H. Mori, H. Fujita, Phil. Mag. B 61 (1990) 107.
[14] A. Matsunaga, C. Kinoshita, K. Nakai, Y. Tomokiyo, J. Nucl. Mater. 179-181 (1991) 457.
[15] L.L. Snead, To be published (2001).
[16] L.L. Snead, S.J. Zinkle, in: Microstructure Evolution During Irradiation eds. I.M. Robertson et al., MRS Symposium Proceedings vol. 439 (Materials Research Society, Pittsburgh, 1997) p. 595.
[17] C.J. McHargue, J.M. Williams, Nucl. Instrum. Meth. in Phys. B80/81 (1993) 889.
[18] C.J. McHargue, G.C. Farlow, C.W. White, J.M. Williams, B.R. Appleton, H. Naramoto, Mat. Sci. Eng. 69 (1985) 123.
[19] C.J. McHargue, C.S. Yust, J. Amer. Ceram. Soc. 67 (1984) 117.
[20] J. Bentley, L.J. Romana, L.L. Horton, C.J. McHargue, in: eds. G.S. Was, L.E. Rehn, D.M. Follstaedt, in: Phase Formation and Modification by Beam-Solid Interactions, Materials Research Soc., 1992 p. 363.
[21] W. Bolse, J. Conrad, T. Rodle, T. Weber, Surf. Coat. Techn. 74-75 (1995) 927.
[22] V. Heera, J. Stoemenos, R. Kogler, W. Skorupa, J. Appl. Phys. 77 (1995) 2999.
[23] C.J. McHargue, D.L. Joslin, J.M. Williams, Nucl. Instrum. Meth. B 46 (1990) 185.

[24] L.L. Snead, S.J. Zinkle, J.C. Hay, M.C. Osborne, Nucl. Instrum. Meth. in Phys. Res. B 141 (1997) 123.
[25] U. Zammit, K.N. Madjusoodanan, F. Scudieri, F. Mercuri, Phys. Rev. B 49 (1994) 2163.
[26] E. Wendler, A. Heft, W. Wesch, Nucl. Instr. Meth. B 141 (1998) 105.
[27] ASTM., D1505-85. Standard Test Method for Density of Plastics by Density Gradient Technique. 1985.
[28] ASTM., B 193-87 Standard Test Method for Resistivity of Electrical Conductor Materials.
[29] W. Jiang, W.J. Weber, S. Thevuthasan, D.E. McCready, Surface and Interface Analysis 27 (1999) 179.
[30] G.N. VanDenHoven, Z.N. Lang, L. Neisen, Phys. Rev. Lett. 68 (1992) 3714.
[31] W.C. Sinke, T. Warabisaco, M. Miyao, T. Tokuyama, S. Roorda, F. Saris, J. Noncrys. Sol. 99 (1988) 308.
[32] S. Roorda et al., Phys. Rev. B 44 (1991) 3702.
[33] C.N. Waddell, W.G. Spitzer, J.E. Friedrickson, G.K. Hubler, T.A. Kennedy, J Appl. Phys. 44 (1984) 4361.
[34] S. Roorda, S. Doorn, W.C. Sinke, O.M.L.O. Scholte, E.v. Loenen, Phys. Rev. Lett 62 (1989) 1880.
[35] E.P. Donovan, F. Spaepen, J.M. Poate, D.C. Jacobson, Appl. Phys. Lett. 55 (1989) 1516.
[36] G. Muller, S. Kalbitzer, Phil. Mag. B38 (1978) 241.
[37] S. Coffa, F. Priolo, J.M. Poate, S.H. Glarum, Nucl. Instrum. Meth. Res. B80/81 (1993) 603.
[38] S. Coffa, J.M. Poate, D.C. Jacobson, W. Frank, W. Gustin, Phys. Rev. B45 (1992) 8355.
[39] N.F. Mott, E.A. Davis, Electronic Processes in Non-crystalline Materials, Oxford Univ. Press, Oxford, 1979.